

Real-Time Estimation of Transmitted Torque on Each Clutch for Ground Vehicles With Dual Clutch Transmission

Jiwon J. Oh and Seibum B. Choi, *Member, IEEE*

Abstract—This paper mainly focuses on the robust separate estimation of transmitted torque on each clutch of the dual clutch transmission—the task that has not yet been accomplished by previously published efforts. In order to estimate the torque on individual clutches, the observer system is composed of a shaft model-based observer, unknown input observers, and a model reference PI observer. The estimations obtained by each subcomponents are processed together to provide online torque estimation of high accuracy. The proposed estimator requires the following information: speed measurements of engine, input shafts, and wheels, and nominal engine torque information obtained as a function of driver inputs and engine speed. These are already available in the current production cars; hence, no further modification or addition to the vehicle hardware is necessary. To validate the effectiveness of the proposed estimator, experiments using an actual vehicle are conducted with various scenarios. With detailed analysis of the results obtained by the experiments, the proposed dual clutch transmission torque estimator is shown to be apt for real car application.

Index Terms—Clutch torque, dual clutch transmission, estimation, output shaft torque, torque observer.

NOMENCLATURE

ω	Speed.
T	Torque.
J	Inertia.
α_{th}	Throttle angle.
θ	Shaft angle.
k	Torsional stiffness.
b	Torsional damping coefficient.
i_t	Transmission gear ratio.

i_f	Final reduction gear ratio.
$\hat{\bullet}$	Estimation.
\bullet_e	Engine.
\bullet_d	Damper.
\bullet_c	Clutch.
\bullet_t	Transfer shaft.
\bullet_o	Output.
\bullet_w	Wheel.
\bullet_v	Vehicle.
\bullet_1	First clutch.
\bullet_2	Second clutch.

I. INTRODUCTION

NOWADAYS, along with the efforts to invent novel transmission systems for various types of vehicles [1]–[5] to improve their performance, the dual clutch transmission (DCT) is emerging as an innovative and useful technology to solve the issues—driving inconvenience or low fuel efficiency—of the conventional manual or automatic transmissions in ground vehicles. This emerging technology has the potential to improve the fuel efficiency, reinforce the gear shift performance, and maintain the convenience of the automatic transmission simultaneously. Such benefits can be obtained by using two clutches that engage alternately during the gear shifts to give efficient and seamless torque transmission. The general description on the DCT can be found in [6].

The sophisticated principles and mechanisms of dual clutch transmissions alone, however, cannot guarantee resolving the previously mentioned limitations of other types of transmissions; they must be supported by effective algorithms to control the actuators within the transmission system. Simple open-loop control tactics based on the experimentally obtained map of the relationship between the actuation input and the clutch torque or speed is insufficient in eliminating the jerks in shift shock [7], [8] and transmission life deterioration.

For robust and efficient actuation of the clutch actuators, real-time feedback control structure is required. However, most of the conventional dry DCT clutch actuator controllers operate position-based. Due to the high torque-to-position ratio, which saves actuation energy, torque control merely based on the actuator position information degrades the launching and gear shift performances, especially in the presence of clutch wear and temperature variation when the empirically obtained position–torque map is no longer reliable. Hence, with the torque

Manuscript received August 8, 2013; revised December 18, 2013; accepted February 19, 2014. Date of publication March 10, 2014; date of current version October 3, 2014. Recommended by Technical Editor G. Herrmann. This work was supported by a National Research Foundation of Korea (NRF) grant funded by the Korea Government (MEST) (2012-0000991) and Global Ph.D. Fellowship Program, and the Ministry of Knowledge Economy (MKE), Korea, under the Convergence Information Technology Research Center (CITRC) support program (NIPA-2012-H0401-12-2003) supervised by the National IT Industry Promotion Agency (NIPA). This work was also supported in part by Valeo Pyeong-Hwa, by which the test vehicle equipped with the DCT hardware, the corresponding TCU commands, and actuator controller was sponsored.

The authors are with Korea Advanced Institute of Science and Technology (KAIST), Daejeon 305-701, Korea (e-mail: jwo@kaist.ac.kr; sbchoi@kaist.ac.kr).

Color versions of one or more of the figures in this paper are available online at <http://ieeexplore.ieee.org>.

Digital Object Identifier 10.1109/TMECH.2014.2307591

monitoring ability for each clutch, improvements in clutch actuation performance including the minimization of shifting time, jerk, and clutch damage, are expected. In addition, less dependency on the actuator position for control can increase the clutch torque-to-position ratio, which can further save actuation energy.

Unfortunately, however, using torque measuring devices on all production cars is not desirable due to their high costs, especially the sensors that have the accuracy that is sufficiently high to ensure improved clutch control performance. This leads to the needs for the estimators that are capable of identifying the clutch torque at no additional cost.

Previous attempts to realize such estimator have been made for the application on the automatic transmission or automated manual transmission (AMT). However, there is no previous work on the development of the individual clutch torque observer for DCTs yet. Turbine torque estimation methods are introduced in [9]–[11], but they cannot be applied on DCT, since the torque converter in the automatic transmission is structurally different from the clutches in DCT. For the torque estimation for AMTs, Kalman filter-based observers are designed [12]–[15], whose estimation performance is limited by the linearized models. The Luenberger observer-based estimation schemes [16], [17] overlooked the effects of the nominal engine torque and vehicle inertia uncertainties. Also, the sliding mode observer in [18] and unknown input observers proposed in [19], [20] involve chattering and phase lag issues. After all, these estimators are applicable only for AMTs, and a novel estimator must be developed to effectively estimate the individual clutch torque for DCTs that are equipped with an additional clutch and transfer shaft when compared with AMTs. In fact, the torque estimation methods for DCTs have been developed as well [21]–[24]. However, their application is only confined to DCT launch control, in which only a single clutch is involved. This implies that the applicability of these estimators is technically the same as that of the aforementioned estimators for AMTs. Torque curve adaptation for DCT actuators using sliding mode observer compensation is proposed in [25], and actuator control tactics are presented in [26], [27], but they still are largely based on the position–torque model that does not guarantee high estimation accuracy in all clutch phases.

Hence, the suggested estimator proposes the unparalleled method to identify the individual clutch torque of both clutches of the DCT system, which continuously function at all times while the vehicle is running. Such ability to monitor clutch torque can enhance the clutch actuation quality, even for the cases with short clutch actuation stroke [28], [29]. The organization of the paper is as follows. Section II-A first describes a model reference PI observer. Sections II-B and C deal with the principles behind an engine dynamics-based unknown input observer, and a clutch dynamics-based unknown input observer designed for two transfer shafts in DCT, respectively. Section II-D focuses on a transfer shaft model-based observer, and Section II-E deals with the signal processing of the observer estimations to effectively handle the gear selection processes. Section III displays the results of the experimental validation conducted

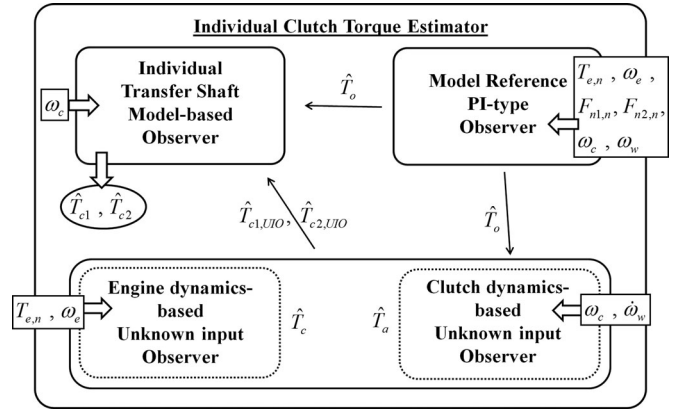


Fig. 1. Schematics of the individual clutch torque observer system.

to show the torque estimation performance, and analyzes the results in detail.

II. CLUTCH TORQUE ESTIMATOR

As the main objective of this study focuses on the estimation of the individual clutch torque in DCTs—a task that has not yet been accomplished in the past—this chapter first introduces the basic structure of the estimator system.

Shown in Fig. 1 are the subcomponents of the clutch torque estimator, which are fused together to give the final estimation of the torque transmitted through the first clutch (henceforth referred to as the clutch 1) and the second clutch (clutch 2), separately.

With the provision of the output torque corrections obtained by the model reference PI-type observer, the two unknown input observers calculate the clutch torque estimations of each side with high reliability during the steady state but with phase lag error during the transient state. On the other hand, the individual transfer shaft model-based observer estimations swiftly respond during the transient states, while they involve drift issue during the steady state. Hence, these observers compensate the weakness of each other to give the clutch torque estimations that are robust both during the steady state and transient state.

The option of partially using the above-mentioned observer system—for instance, only the unknown input observers—are also available to reduce the computational load when applied on a real vehicle, but the experiment results—to be displayed in the later part—show that the current system is sufficient for the real-time application of the suggested observer.

Details on the designs of each subobserver are presented in the following sections. It must be noted that the states dealt in each parts are independent of the corresponding states in others, except the interconnecting states: \hat{T}_o , \hat{T}_a , \hat{T}_c , $\hat{T}_{c1,UIO}$, and $\hat{T}_{c2,UIO}$.

A. Model Reference PI Observer

The main objective for the model reference PI observer is to estimate the output shaft torque so that this estimation can be used in the clutch dynamics-based unknown input observer and individual transfer shaft model-based observer.

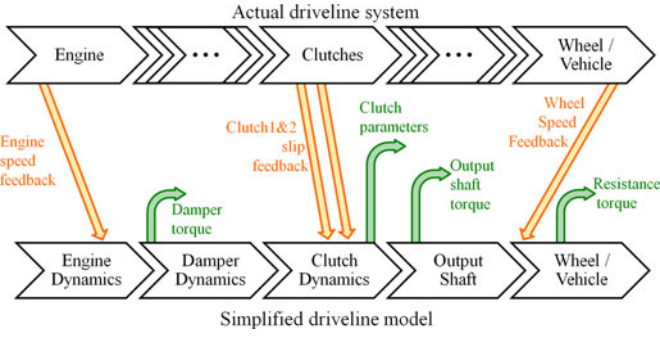


Fig. 2. Conceptual diagram of the operation principles of the model reference PI observer.

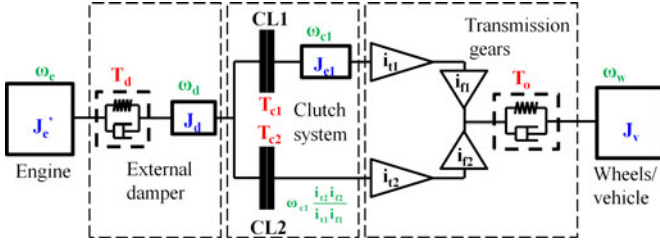


Fig. 3. Simplified driveline model of the dual clutch transmission system (J : inertia, T : torque, w : angular velocity).

The PI observer is based on the model of driveline, which uses the predefined parameters such as the nominal engine torque information mapped against the throttle input and engine speed, inertia of the shafts and gears, gear ratio, and torsional stiffness and damping coefficients. Although the developed model may be able to approximately resemble the actual driveline, it is highly demanding to consider every aspect of the driveline accurately due to high complexity and computational load. Thus, the model reference PI observer estimates the states (especially the output shaft torque estimation for which the model reference PI observer is designed) whose measurements are unavailable (rising arrows in Fig. 2), based on the model that is deliberately designed to follow the actual driveline states by using the measurement feedback (descending arrows in Fig. 2). This effectively operates as a correction for the unaccounted uncertainties and errors in the nominal system such as the gear backlash and tire dynamics.

Before dealing with the observer design, the driveline model used for this observer is briefly introduced in the following.

1) *Driveline Model for Model Reference PI Observer*: The driveline model used for the model reference PI observer to describe the flow of the torque from the engine to the wheels through the dual clutch transmission can be basically shown as follows.

Using the torque balance relationships, the driveline model shown in Fig. 3 can be mathematically represented as shown by

$$J'_e \dot{\omega}_e = T_e - T_d \quad (1)$$

where J'_e denotes the engine inertia only, independent from the inertia of the external damper.

The torsional damper, often in the form of a dual mass fly-wheel, isolates the vehicle from the engine's torsional vibration by using the two masses each connected to the engine and the transmission, that are linked by the spring damper system. The torque balance relationship of the engine and the torsional damper is shown in (1). Modeling of the torsional damper can be optionally included, or otherwise the engine torque can directly express the damper output torque

$$J_d \dot{\omega}_d = T_d - T_{c1} - T_{c2} \quad (2)$$

$$J_{e1} \dot{\omega}_{c1} = T_{c1} + T_{c2} \frac{i_{t2} i_{f2}}{i_{t1} i_{f1}} - \frac{T_o}{i_{t1} i_{f1}}. \quad (3)$$

The clutch 1 dynamics shown in (3) can be expressed from the perspective of clutch 2, as shown by

$$J_{e2} \dot{\omega}_{c2} = T_{c1} \frac{i_{t1}}{i_{t2}} + T_{c2} - \frac{T_o}{i_{t2}} \quad (4)$$

$$J_v \dot{\omega}_w = T_o i_f - T_v. \quad (5)$$

Here, J_{e1} and J_{e2} refer to the effective transmission inertia from clutch 1 and 2 perspective, respectively, and the wheel speed refers to the processed rotational speed that can be obtained by assuming that no speed difference exists between the two ends of the differential gear. For each dynamics, the related torque is modeled as follows:

$$T_e = f(\alpha_{th}, \omega_e) \quad (6)$$

$$T_d = k_d (\theta_e - \theta_d) + b_d (\omega_e - \omega_d) \quad (7)$$

$$T_{c1} = F_{n1} C_{c1} \mu \text{sgn}(\omega_d - \omega_{c1}) \quad (8)$$

$$T_{c2} = F_{n2} C_{c2} \mu \text{sgn}(\omega_d - \omega_{c2}) \quad (9)$$

$$T_o = k_o \left(\frac{\theta_c}{i_t} - i_f \theta_w \right) + b_o \left(\frac{\dot{\omega}_c}{i_t} - i_f \dot{\omega}_w \right) \quad (10)$$

$$T_v = r_w \left(\underbrace{m_v g \sin(\theta_{road})}_{\text{road gradient}} + \underbrace{K_{rr} m_v g \cos(\theta_{road})}_{\text{rolling resistance}} + \underbrace{\frac{1}{2} \rho v_x^2 C_d A}_{\text{aerodynamic drag}} \right). \quad (11)$$

Here, F_n , C_c , m , r_w , q_{road} , K_{rr} , m_v , ρ , v_x , C_d , and A each indicate the clutch normal force, clutch effective area, clutch friction coefficient, wheel radius, road gradient angle, tire rolling resistance, vehicle mass, air density, vehicle velocity, aerodynamic drag coefficient, and vehicle frontal area, respectively. The engine torque (6) is determined based on the empirically obtained relationship between the engine load conditions and produced net torque. The damper torque (7) and the output torque (10) are expressed using the torsional compliance model involving spring constant and damping effect. The clutch torques (8) and (9) are expressed using the simple friction model where the torque is given as a function of clutch normal force and nominal friction coefficient. The vehicle resistance torque (11) is the sum of the effects of road gradient, tire rolling resistance, and aerodynamic drag. Again, please note that the validity of these nominal expressions used for the model reference PI observer

compared to the actual driveline carries less significance, since they are to be compensated using a feedback structure as shown in Fig. 2.

2) *Model Reference PI Observer Structure:* The observer is mainly based on the driveline model introduced in the previous section. The estimated speeds of the engine, external damper, clutch 1 and 2, and wheel are obtained using the following observer equations:

$$\dot{\hat{\omega}}_e = \frac{T_{e,n}}{J_e} - \frac{\hat{T}_d}{J_e} \quad (12)$$

where $T_{e,n}$ is the nominal engine torque

$$\dot{\hat{\omega}}_d = \frac{\hat{T}_d}{J_d} - \frac{\hat{T}_{c1}}{J_d} - \frac{\hat{T}_{c2}}{J_d} \quad (13)$$

$$\dot{\hat{\omega}}_{c1} = \frac{\hat{T}_{c1}}{J_{e1}} + \hat{T}_{c2} \frac{i_{t2}i_{f2}}{J_{e1}i_{t1}i_{f1}} - \frac{\hat{T}_o}{J_{e1}i_{t1}i_{f1}} \quad (14)$$

$$\dot{\hat{\omega}}_{c2} = \hat{T}_{c1} \frac{i_{t1}i_{f1}}{J_{e2}i_{t2}i_{f2}} + \frac{\hat{T}_{c2}}{J_{e2}} - \frac{\hat{T}_o}{J_{e2}i_{t2}i_{f2}} \quad (15)$$

$$\dot{\hat{\omega}}_w = \frac{\hat{T}_o}{J_v} - \frac{\hat{T}_v}{J_v}. \quad (16)$$

Here, (14) and (15) are used separately in dual form to maximize estimation accuracy during gear selection, which is dealt in the signal processing section. It can be checked here that each observer dynamics from (12) to (16) directly bases on the simplified driveline model equations indicated from (1) to (5), respectively. These observer equations require the estimated torque besides the model parameters. Here, the proportional and integral state feedback terms are included in the torque calculation, so that each estimated state variable of the model-based observer can converge to the actual states of the driveline

$$\hat{T}_d = k_d (\hat{\theta}_e - \hat{\theta}_d) + b_d (\hat{\omega}_e - \hat{\omega}_d) - L_{dp} \dot{\hat{\theta}}_e - L_{di} \tilde{\theta}_e \quad (17)$$

$$\dot{\hat{\theta}}_e = \omega_e - \hat{\omega}_e. \quad (18)$$

The engine speed feedback is used for the estimation of the torque transmitted through the external damper as shown in (17). This is physically reasonable since underestimation of the engine speed naturally implies overestimation of the external damper torque

$$\hat{T}_{c1} = F_{n1} C_{c1} \mu \text{sgn}(\hat{\omega}_d - \hat{\omega}_{c1}) - L_{c1p} \dot{\hat{\theta}}_{s1} - L_{c1i} \tilde{\theta}_{s1} \quad (19)$$

$$\dot{\hat{\theta}}_{s1} = (\omega_d - \omega_{c1}) - (\hat{\omega}_d - \hat{\omega}_{c1}) \quad (20)$$

$$\hat{T}_{c2} = F_{n2} C_{c2} \mu \text{sgn}(\hat{\omega}_d - \hat{\omega}_{c2}) - L_{c2p} \dot{\hat{\theta}}_{s2} - L_{c2i} \tilde{\theta}_{s2} \quad (21)$$

$$\dot{\hat{\theta}}_{s2} = (\omega_d - \omega_{c2}) - (\hat{\omega}_d - \hat{\omega}_{c2}). \quad (22)$$

Similar to the external damper torque estimation, clutch torque estimation involves the clutch slip feedback. Such maneuver is also reasonable, since underestimation of the clutch slip naturally implies overestimation of the friction between the clutch plates, and thus overestimation of the clutch torque. Although \hat{T}_{c1} and \hat{T}_{c2} are not interconnecting variables directly

used in other subobservers, they indirectly contribute in the computation of \hat{T}_o , an interconnecting variable

$$\hat{T}_o = k_o \left(\frac{\hat{\theta}_{c1}}{i_{t1}i_{f1}} - \hat{\theta}_w \right) + b_o \left(\frac{\hat{\omega}_{c1}}{i_{t1}i_{f1}} - \hat{\omega}_w \right). \quad (23)$$

Instead of adding a feedback term for the output shaft torque estimation, the wheel speed feedback is included in the estimation of the resistance torque of the vehicle as shown in (24), so that the effects due to unknown disturbances such as braking torque, varying road gradient, or wind can be accounted in the estimation of \hat{T}_v . This way, the output shaft torque estimation, which is the main objective for this subobserver, can remain uninfluenced by the disturbances

$$\begin{aligned} \hat{T}_v = r_w \left(\underbrace{m_v g \sin(\theta_{\text{road}})}_{\text{road gradient}} + \underbrace{K_{rr} m_v g \cos(\theta_{\text{road}})}_{\text{rolling resistance}} \right. \\ \left. + \underbrace{\frac{1}{2} \rho v_x^2 C_d A}_{\text{aerodynamic drag}} \right) - L_{wp} \dot{\hat{\theta}}_w - L_{wi} \tilde{\theta}_w \end{aligned} \quad (24)$$

$$\dot{\hat{\theta}}_w = \omega_w - \hat{\omega}_w. \quad (25)$$

Since the proposed observer is based on the principle of simple PI-type feedback observer using the measurement terms, the convergence to the measured values is obvious and the stability analysis is omitted.

Also, instead of depending on the clutch 1 dynamics for the estimation of the output shaft speed in (23), the clutch 2 dynamics can be applied as well. The advantage of considering both cases is dealt in the later part about signal processing.

B. Engine Dynamics-Based Unknown Input Observer

The main objective for the engine dynamics-based unknown input observer (UIO) is to estimate the combined clutch 1 and clutch 2 torque. Thus, the estimation target of the observer is defined as follows:

$$T_c \equiv T_{c1} + T_{c2}. \quad (26)$$

Now, recall the engine dynamics stated in (2). With the dynamics of the torsional damper considered negligible, we have

$$J_e \dot{\omega}_e = T_e - T_{c1} - T_{c2} \quad (27)$$

$$\dot{\omega}_e = \frac{T_e}{J_e} - \frac{T_{c1}}{J_e} - \frac{T_{c2}}{J_e} \quad (28)$$

where J_e denotes the lumped engine and damper inertia. Based on (28), the observer is designed as shown by

$$\dot{\hat{\omega}}_e = \frac{1}{J_e} T_{e,n} - \frac{1}{J_e} \hat{T}_c + l_1 (\omega_e - \hat{\omega}_e) \quad (29)$$

$$\dot{\hat{T}}_c = -l_2 (\omega_e - \hat{\omega}_e). \quad (30)$$

The stability of the engine dynamics-based unknown input observer error can easily be shown under the assumption that the externally obtained variable is indeed close to the actual state; hence, the analysis is omitted.

Conventional clutch torque observer for the transmission with just a single clutch (AMT) shown recent works [30], [31] uses the simplified version of (27) to estimate the clutch torque. However, such method alone shows limited performance due to the engine torque inaccuracy and phase lag issue; most of all, such estimator cannot be applied to the DCT.

To make it applicable for DCT, the estimation of \hat{T}_c is later used together with the estimations obtained by the clutch dynamics-based unknown input observer, which is introduced in the following section.

C. Clutch Dynamics-Based Unknown Input Observer

Similar to the case of engine dynamics-based unknown input observer, the main objective of the clutch dynamics-based unknown input observer is to estimate combined clutch 1 and clutch 2 torques represented from the perspective of clutch 1. Hence, the estimation target is defined as follows:

$$T_{a1} \equiv T_{c1} + \frac{\dot{i}_{t2}\dot{i}_{f2}}{\dot{i}_{t1}\dot{i}_{f1}}T_{c2}. \quad (31)$$

Now, recall the clutch dynamics dealt in (3). Here, the clutch 1 speed is isolated to give the following relationship:

$$\dot{\omega}_{c1} = \frac{T_{c1}}{J_{e1}} + \frac{\dot{i}_{t2}\dot{i}_{f2}}{J_{e1}\dot{i}_{t1}\dot{i}_{f1}}T_{c2} - \frac{T_o}{J_{e1}\dot{i}_{t1}\dot{i}_{f1}}. \quad (32)$$

Based on this, the unknown input observer is designed, as shown by

$$\dot{\hat{\omega}}_{c1} = \frac{1}{J_{12,1}}\hat{T}_{a1} - \frac{\hat{T}_o}{J_{12,1}\dot{i}_{t1}\dot{i}_{f1}} + l_3(\omega_{c1} - \hat{\omega}_{c1}) \quad (33)$$

$$\dot{\hat{T}}_{a1} = l_4(\omega_{c1} - \hat{\omega}_{c1}). \quad (34)$$

As it can be seen in (33), the clutch dynamics-based unknown input observer requires the output shaft torque information. This output shaft torque is substituted by the output shaft torque estimation obtained in the model reference PI observer in (23).

Now, that both \hat{T}_c and \hat{T}_{a1} are estimated, these values can be fused together to give the rough estimation of the clutch 1 torque and clutch 2 torque, and these rough estimations can be expressed as follows:

$$\hat{T}_{c1,1} \equiv \frac{\dot{i}_{t1}\dot{i}_{f1}\hat{T}_{a1} - \dot{i}_{t2}\dot{i}_{f2}\hat{T}_c}{\dot{i}_{t1}\dot{i}_{f1} - \dot{i}_{t2}\dot{i}_{f2}} \quad (35)$$

$$\hat{T}_{c2,1} \equiv \frac{\dot{i}_{t1}\dot{i}_{f1}\hat{T}_c - \dot{i}_{t1}\dot{i}_{f1}\hat{T}_{a1}}{\dot{i}_{t1}\dot{i}_{f1} - \dot{i}_{t2}\dot{i}_{f2}}. \quad (36)$$

Here, the subscripts $c1$ and $c2$ imply clutch 1 and clutch 2, respectively, and the number after it tells that the estimation is based on the unknown input observer derived with clutch 1 perspective.

Of course, the clutch dynamics-based unknown input observer can also be designed using the clutch 2 dynamics as well by defining the estimation target as shown by

$$T_{a2} \equiv \frac{\dot{i}_{t1}\dot{i}_{f1}}{\dot{i}_{t2}\dot{i}_{f2}}T_{c1} + T_{c2}. \quad (37)$$

The observer equations would have to be altered accordingly so that they are based on the clutch 2 dynamics.

Such alternative option can be useful for the application on actual vehicles when the gear selector is shifting on the first transfer shaft that involves a discrete change in inertia. Further detail on this is dealt in the signal processing section.

Similar to how rough estimations of clutch torques were obtained in (35) and (36) by using \hat{T}_c and \hat{T}_{a1} , the following shows the expression of the individual clutch torques obtained by using \hat{T}_c and \hat{T}_{a2} , the output from the engine dynamics-based unknown input observer and the second version of the clutch dynamics-based unknown input observer with the clutch 2 perspective

$$\hat{T}_{c1,2} \equiv \frac{\dot{i}_{t2}\dot{i}_{f2}\hat{T}_c - \dot{i}_{t2}\dot{i}_{f2}\hat{T}_{a2}}{\dot{i}_{t2}\dot{i}_{f2} - \dot{i}_{t1}\dot{i}_{f1}} \quad (38)$$

$$\hat{T}_{c2,2} \equiv \frac{\dot{i}_{t2}\dot{i}_{f2}\hat{T}_{a2} - \dot{i}_{t1}\dot{i}_{f1}\hat{T}_c}{\dot{i}_{t2}\dot{i}_{f2} - \dot{i}_{t1}\dot{i}_{f1}}. \quad (39)$$

The individual clutch torque estimations ($\hat{T}_{c1,UIO}$ and $\hat{T}_{c2,UIO}$ from signal processing of $\hat{T}_{c1,1}$, $\hat{T}_{c1,2}$, $\hat{T}_{c2,1}$, and $\hat{T}_{c2,2}$) are interconnecting states used in the individual transfer shaft model-based observer. $\hat{T}_{c1,UIO}$, and $\hat{T}_{c2,UIO}$ are merely considered as the interim results, because the unknown input observers involve the phase lag issue by their nature, and also because the driveline model used to derive the observer equations was overly simplified. On the other hand, such nature provides the strong advantage of robustness and stability at steady states.

Hence, these clutch torque estimations obtained by the unknown input observers are designed to assist the individual transfer shaft model-based observer to obtain the final estimation result, which is dealt in the following section.

D. Individual Transfer Shaft Model-Based Observer

Whenever a shaft experiences torsional effort, its compliance causes angular deflection. Such compliance of each transfer shaft can be modeled, and the individual transfer shaft model-based observer uses this model to identify each clutch torque separately. Such tactics enable the estimation of individual clutch torque with higher accuracy than that obtained solely by the unknown input observers. To present the details of the individual transfer shaft model-based observer, a DCT driveline model including the transfer shaft compliance is introduced.

1) *DCT Driveline Model with Transfer Shaft Compliance*: While the driveline model previously introduced for the design of the model reference PI observer has the strength of simplicity, it involves the weakness of limited accuracy for representing internal dynamics such as shaft compliance and backward torque recirculation. Hence, the transfer shaft compliance is modeled to form the driveline model shown in Fig. 4, on which the individual transfer shaft model-based observer is designed.

For this model, instead of considering the transmission dynamics as a function the clutch torque and output shaft torque,

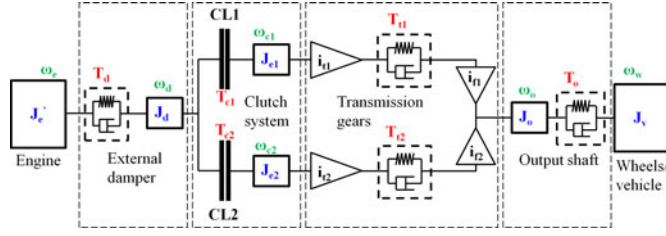


Fig. 4. Driveline model of the dual clutch transmission system that involves transfer shaft compliance (J : inertia, T : torque, w : angular velocity).

it is described as a function of the transfer shaft torque

$$J_{c1}\dot{\omega}_{c1} = T_{c1} - \frac{T_{t1}}{i_{t1}} \quad (40)$$

$$J_{c2}\dot{\omega}_{c2} = T_{c2} - \frac{T_{t2}}{i_{t2}}. \quad (41)$$

This alters the output shaft dynamics as the following:

$$J_o\dot{\omega}_o = i_{f1}T_{t1} + i_{f2}T_{t2} - T_o. \quad (42)$$

Each torque in these torque balance relationships can be then replaced by the following expressions for the transfer shaft and output shaft torques

$$T_{t1} = k_{t1} \left(\frac{\theta_{c1}}{i_{t1}} - i_{f1}\theta_o \right) + b_{t1} \left(\frac{\omega_{c1}}{i_{t1}} - i_{f1}\omega_o \right) \quad (43)$$

$$T_{t2} = k_{t2} \left(\frac{\theta_{c2}}{i_{t2}} - i_{f2}\theta_o \right) + b_{t2} \left(\frac{\omega_{c2}}{i_{t2}} - i_{f2}\omega_o \right) \quad (44)$$

$$T_o = k_o (\theta_o - \theta_w) + b_o (\omega_o - \omega_w). \quad (45)$$

The key of the driveline model used for the individual transfer shaft model-based observer is to model each transfer shaft separately, so that the torques transmitted through each transfer shaft can be expressed as shown in (43) and (44). The remaining parts of the driveline model can be constructed in the similar manner as those of the previously mentioned simplified driveline model accordingly.

2) *Individual Transfer Shaft Model-Based Observer Structure*: In the individual transfer shaft model-based observer design procedures, it is assumed that the effective shaft inertia and the output shaft inertia are small enough to be neglected for the noise rejection purpose. Such assumption does not deteriorate the observer performance since they are indeed much smaller than the engine and the vehicle inertia, and those neglected here can be treated as part of the vehicle inertia eventually because the relative deflections among the transmission parts, shafts, and wheels are considerably small due to high stiffness. This assumption, however, does not imply that the transfer shaft compliance can be neglected as well. The individually modeled transfer shaft compliance plays the key role in the accurate identification of each clutch torque.

Based on the assumption made earlier and the clutch dynamics modeled in (40) and (41), we have the following approximation of the clutch torques:

$$i_{t1}T_{c1} \approx T_{t1} \quad (46)$$

$$i_{t2}T_{c2} \approx T_{t2}. \quad (47)$$

Also, the following equality between the sum of transfer shaft torques and the output shaft torque can be deduced:

$$T_o \approx i_{f1}T_{t1} + i_{f2}T_{t2}. \quad (48)$$

Now, from (17) and (18), we have the following expressions for the clutch torques, knowing that the shaft torsional damping is small enough to be negligible

$$T_{c1} = \frac{k_{t1}}{i_{t1}} \left(\frac{\theta_{c1}}{i_{t1}} - i_{f1}\theta_o \right) \quad (49)$$

$$T_{c2} = \frac{k_{t2}}{i_{t2}} \left(\frac{\theta_{c2}}{i_{t2}} - i_{f2}\theta_o \right). \quad (50)$$

To attempt estimation of clutch torques by using (49) and (50), the output shaft angle is required. Here, however, since the feedback term is to be added in the form of a Luenberger observer to guarantee convergence toward the actual state, availability of the output shaft speed is preferred over the output shaft angle. So the clutch observer is to be designed based on the following:

$$\dot{T}_{c1} = \frac{k_{t1}}{i_{t1}} \left(\frac{w_{c1}}{i_{t1}} - i_{f1}w_o \right) \quad (51)$$

$$\dot{T}_{c2} = \frac{k_{t2}}{i_{t2}} \left(\frac{w_{c2}}{i_{t2}} - i_{f2}w_o \right). \quad (52)$$

Hence, we see that the estimation of the output shaft speed is required for the estimation of the clutch torques. To estimate the output shaft speed, (49) and (50) are substituted into (48) using (46) and (47) to reach the following:

$$T_o = k_{t1}i_{f1} \left(\frac{\theta_{c1}}{i_{t1}} - i_{f1}\theta_o \right) + k_{t2}i_{f2} \left(\frac{\theta_{c2}}{i_{t2}} - i_{f2}\theta_o \right). \quad (53)$$

Now, taking the derivative of (53) gives the following:

$$\dot{T}_o = k_{t1}i_{f1} \left(\frac{\omega_{c1}}{i_{t1}} - i_{f1}\omega_o \right) + k_{t2}i_{f2} \left(\frac{\omega_{c2}}{i_{t2}} - i_{f2}\omega_o \right). \quad (54)$$

This is altered to isolate the output shaft speed as shown by

$$\omega_o = \frac{k_{t1}i_{f1}(\omega_{c1}/i_{t1}) + k_{t2}i_{f2}(\omega_{c2}/i_{t2}) - \dot{T}_o}{k_{t1}i_{f1}^2 + k_{t2}i_{f2}^2}. \quad (55)$$

One may argue about the validity of clutch torque observer based on (51) and (52), since the difference between the measured clutch 1 and clutch 2 speeds each multiplied by appropriate gear ratios may be trivial. Hence, to verify the potential to identify each clutch torque using two transfer shaft compliances, open-loop integration of (51) and (52) is taken to check if the result shows any meaningful shape, and it is plotted in Fig. 5.

Here, the measured output shaft torque was used to replace the output shaft torque rate in (55), which caused excessive noise. This would not be problematic for the case of the actual observer to be designed, since output shaft torque information obtained by the model reference PI observer is used instead of using the direct differentiation of the output shaft torque measurement. As shown in the plot, the result indeed shows the rise and fall of the clutch torques effectively as each clutch engages and disengages. It must be noted that the map-based torques do not represent the actual clutch torque, since they are merely

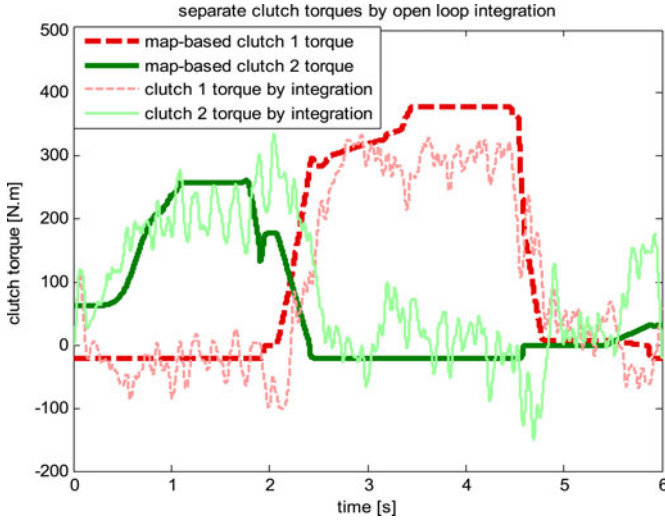


Fig. 5. Open-loop integration of clutch torque rates based on the transfer shaft compliance models.

obtained based on the predefined relationship between the actuator position and the steady state torque. Still, however, the coherence between the clutch torques obtained by two different methods implies that identifying clutch torques through transfer shaft model is feasible.

To obtain the estimated output shaft speed in the actual observer, the output shaft torque can be replaced by that obtained by the model reference PI observer, and the following estimator for the output shaft speed can be derived:

$$\hat{\omega}_o = \frac{k_{t1} i_{f1} (\omega_{c1,m} / i_{t1}) + k_{t2} i_{f2} (\omega_{c2,m} / i_{t2}) - \dot{\hat{T}}_o}{k_{t1} i_{f1}^2 + k_{t2} i_{f2}^2}. \quad (56)$$

Now, by using the estimated output shaft speed, the following individual clutch torque observer is designed:

$$\dot{\hat{T}}_{c1} = \frac{k_{t1}}{i_{t1}} \left(\frac{\omega_{c1,m}}{i_{t1}} - i_{f1} \hat{\omega}_o \right) + L_1 \left(\hat{T}_{c1,UIO} - \hat{T}_{c1} \right) \quad (57)$$

$$\dot{\hat{T}}_{c2} = \frac{k_{t2}}{i_{t2}} \left(\frac{\omega_{c2,m}}{i_{t2}} - i_{f2} \hat{\omega}_o \right) + L_2 \left(\hat{T}_{c2,UIO} - \hat{T}_{c2} \right) \quad (58)$$

where $\hat{T}_{c1,UIO}$ and $\hat{T}_{c2,UIO}$ are the initial estimations of clutch torques obtained by using the unknown input observers and L_1 and L_2 are feedback gains. Through synthesizing the clutch torque estimations obtained by the unknown input observers and those based on the transfer shaft compliance model, the observer achieves high estimation accuracy both in transient and steady states.

To show the internal processes within the observer, Fig. 6 compares the estimated output shaft speed along with the sensor speed measurements and processed clutch torque estimation. Rows (a) and (b) of Fig. 6 show the increasing or decreasing clutch torques. As it can be anticipated, row (c) indeed shows that the input shaft speed measurement is generally greater than the estimated output shaft speed when the clutch torque of the relevant side is increasing, and that the speed measurement is generally lower than the estimated output shaft speed when the

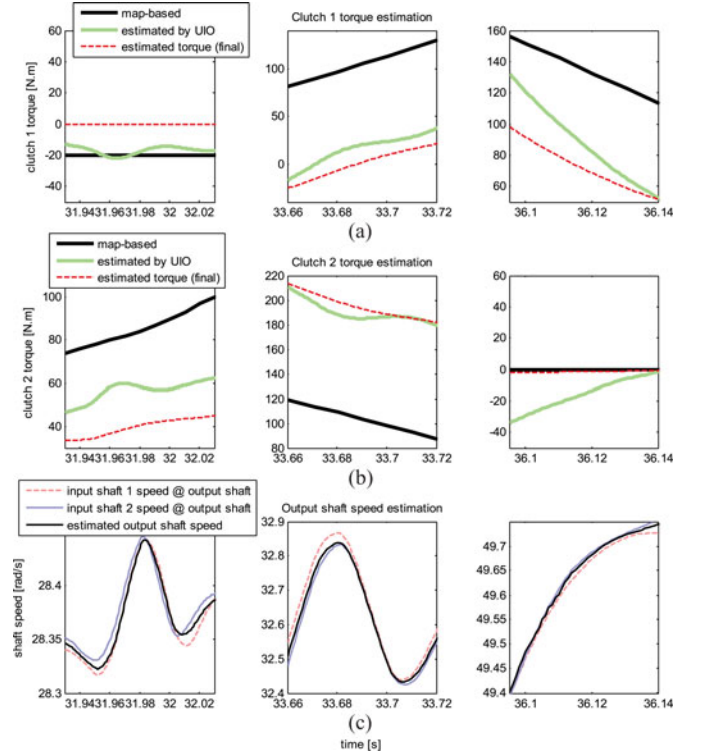


Fig. 6. Individual transfer shaft model-based observer states: (a) clutch 1 torques, (b) clutch 2 torques, and (c) output shaft speed estimation along with input shafts 1 and 2 speed measurements calibrated by gear ratio.

clutch torque of the relevant side is decreasing. Here, the input shaft speed measurements are corrected by the factor of relevant gear ratio so that they can be compared with the estimated output shaft speed. The individual transfer shaft model-based observer takes a Luenberger-like form, and thus the stability analysis is considered obvious. Moreover, to experimentally verify the estimation performance of the entire system, it is thoroughly analyzed and verified by applying to a real vehicle in the following chapter.

E. Signal Processing

Signal processing of the observer estimations is crucial for the elimination of noise without damaging the estimation performance, and also for prevention of unnecessary dependence on the observer.

1) *Observer Signal Processing During Gear Selection:* As shown in Fig. 7(a), gear shifts frequently take place while driving a vehicle, and the desired gear on the input shaft with the disengaged clutch is preselected between each gear shifts. Such characteristic of DCTs involves sudden discontinuity of gear ratio, and it can cause frequent jumps in the estimation results obtained by the observer.

The individual transfer shaft model-based observer is the least affected by the gear ratio discontinuity, since it does not involve direct feedback of the clutch speeds. It is, however, the function of gear ratios, whose sudden change may generate noise.

Hence, instead of switching to the predefined gear ratio directly with each gear selection, the lumped gear ratio values

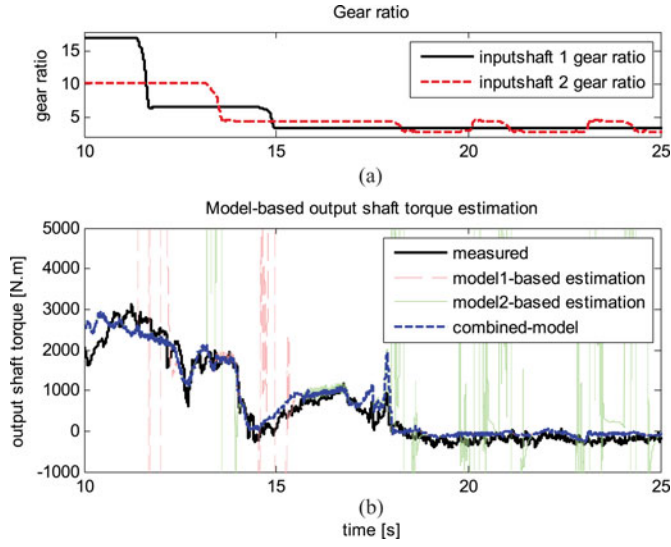


Fig. 7. Plot of the model reference PI observer estimation results: (a) gear ratio changes and (b) output shaft torque estimation.

are deliberately replaced momentarily by the quotient of the measured clutch speed and processed wheel speed, so that the current gear ratio can be switched to the target gear ratio rather smoothly. These processed gear ratios are plotted in row (a) of Figs. 7 and 9.

Unlike the case of the transfer shaft model-based observer, other subobservers are rather critically influenced by the gear ratio jumps, since they use the clutch speed measurements directly in their feedback terms. This problem can be eliminated effectively by using the dual models in case of the model reference PI observer. Exploiting the characteristic of DCTs that gear selections do not take place simultaneously at both shafts, dual versions of the proposed observer—one designed based on the clutch 1 dynamics as shown in (23) and another based on the clutch 2 dynamics—can be built so that the observer of the side without gear ratio jumps can be used.

It can be clearly seen in Fig. 7 that only the estimated states obtained by the observer based on the clutch 1 dynamics fluctuate when the gear ratio on the side of input shaft 1 changes, whereas only those obtained by the observer based on the clutch 2 dynamics fluctuate when the gear ratio on the side of input shaft 2 changes.

Thus, by combining the dual models using the TCU command, the output shaft torque estimation that is robust against gear selection disturbance can be achieved.

The same principle can be applied for the case of the unknown input observer as well. Dual versions for the clutch dynamics-based unknown input observers—one designed based on the clutch 1 dynamics as shown in (33) and (34) and another based on the clutch 2 dynamics—can be built so that the observer of the side without gear ratio jumps can be used.

Similar to the case of model reference PI observer, Fig. 8 clearly shows that fluctuation in the clutch torque estimation obtained by unknown input observer can be eliminated through combination of the estimated results obtained by two versions

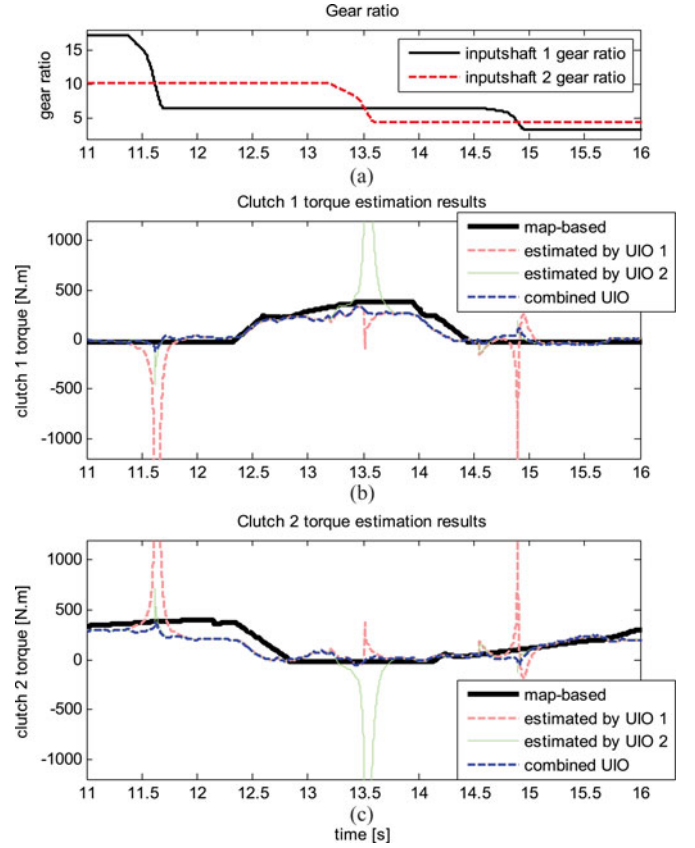


Fig. 8. Plot of the clutch dynamics-based UIO estimation results: (a) gear ratio changes, (b) estimation of clutch 1 torque, and (c) estimation of clutch 2 torque.

of observers: one based on the clutch 1 perspective and the other on clutch 2.

2) *Signal Processing During Clutch Disengaged Phase:* The torque-position characteristic of the clutches varies distinctively with the clutch state, depending on whether the clutch position is beyond or before the kissing point. Here, the kissing point of the clutch refers to the clutch position where the disengaged clutch barely begins to come in contact with the damper plate and slip. Thus, beyond the clutch kissing point it is wiser to monitor the clutch torque itself by using the clutch torque observer rather than to find the torque based on the clutch actuator position. However, before the clutch kissing point when the clutch is in the completely disengaged state, it is much more effective to monitor the clutch position rather than to directly estimate the transmitted torque.

Hence, based on the clutch actuator position information, the clutch torque estimations obtained by the unknown input observers are replaced by zero before they are used as the feedback signal for the transfer shaft model-based observer whenever the clutch is disengaged. Such maneuver ensures the final clutch torque estimation to converge toward zero as well whenever necessary. Even without such processing procedure, the observer system successfully converges toward the actual states. However, the proposed observer is facilitated by the signal processing

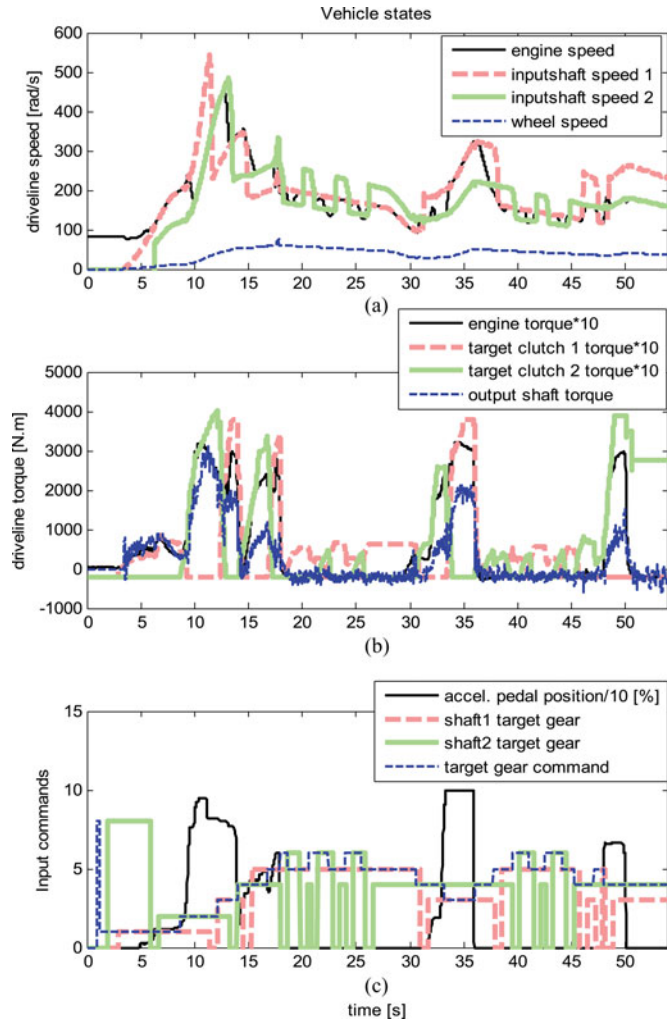


Fig. 9. Experiment scenario: (a) measured driveline speeds, (b) measured torques, (c) driver input and TCU commands—acceleration pedal position is plotted with the scale from 0 to 10 (no to full throttle). TCU target gear command indicates the number of the desired gear from the 1st to 7th, where 0th gear indicates neutral and 8th gear indicates reverse.

methodologies introduced in this section to achieve improved response and noise reduction.

III. EXPERIMENTAL VALIDATION

Ground vehicles operate under various conditions and experience numerous unexpected disturbances. In order to apply the proposed clutch torque estimator on a real vehicle, the estimation performance must be sufficiently robust so that the estimation accuracy is constantly maintained throughout the driving. Hence, the observer must be tested in various conditions as well, so that its effectiveness can be genuinely verified.

A. Test Scenario

The experiment is conducted under the supervision Valeo Pyeong-Hwa, by which the test vehicle with the DCT hardware, the corresponding TCU commands, and actuator controller is arranged.

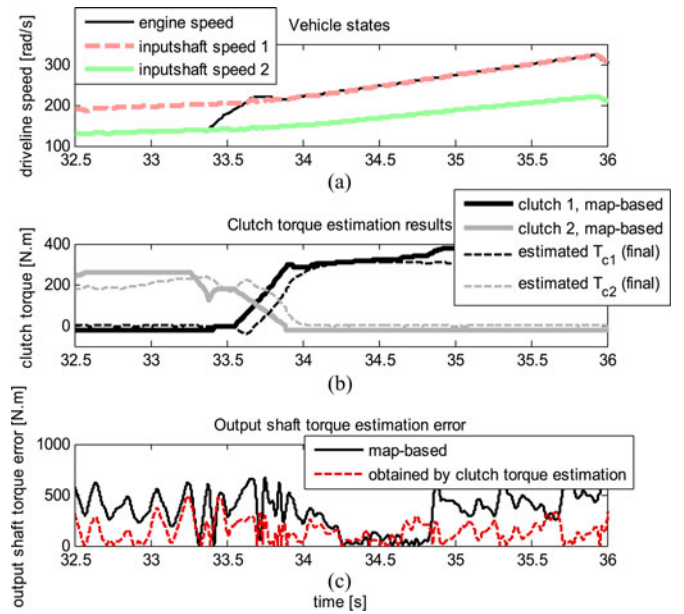


Fig. 10. Individual clutch torque estimation results during gear shift: (a) speed measurements, (b) estimations of clutch 1 and 2 torque, and (c) errors of the output shaft torque estimations.

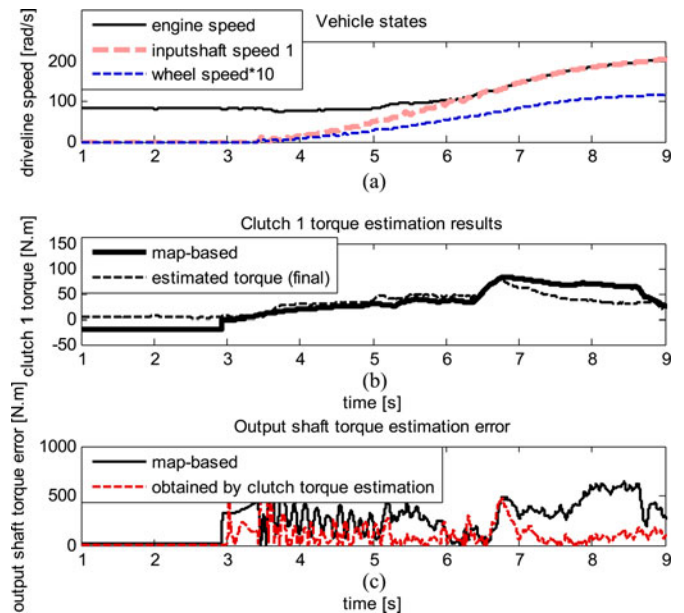


Fig. 11. Individual clutch torque estimation results during launch: (a) speed measurements, (b) estimation of clutch 1 torque, and (c) errors of the output shaft torque estimations.

The test scenario consists of driving the vehicle for approximately 1 min. This scenario includes multiple gear shifts that take place during a kick-down acceleration, moderate acceleration, cruising, deceleration, launching, driving over a speed bump, excessive wheel slip on slippery surface, and fuel cut. Detailed plots of the vehicle states for the test are displayed in Fig. 9, and the estimation results are displayed in Figs. 10–15.

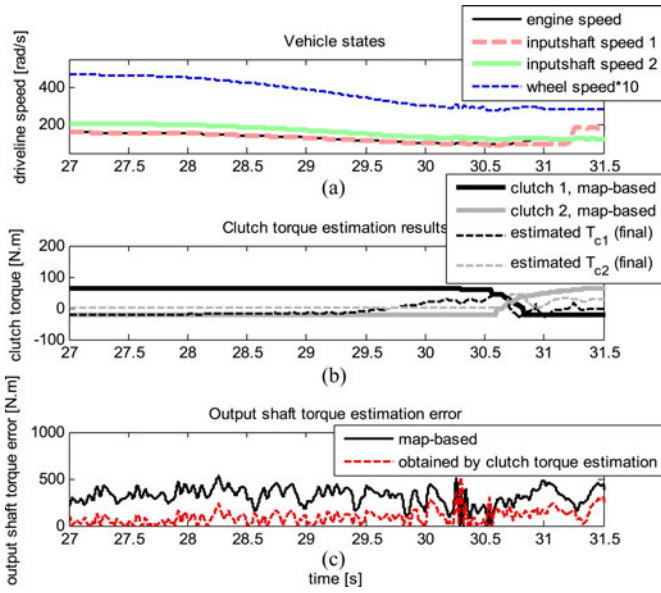


Fig. 12. Clutch torque estimation results during braking and speed bump: (a) speed measurements, (b) estimations of clutch 1 and 2 torque, and (c) errors of the output shaft torque estimations.

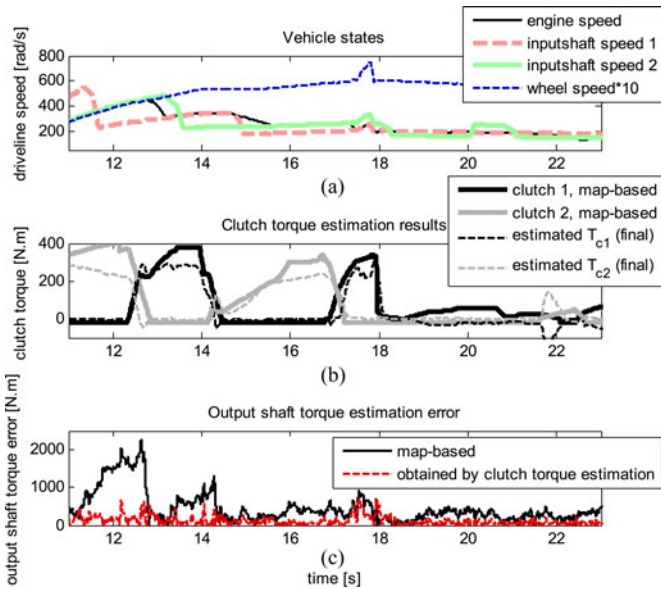


Fig. 13. Individual clutch torque estimation results during wheel slip: (a) speed measurements, (b) estimations of clutch 1 and 2 torque, and (c) errors of the output shaft torque estimations.

B. Test Results

The validation of the clutch torque estimation is indirectly conducted through converting the estimated clutch torque into output shaft torque, so that it can be compared to the measured output shaft torque. Such indirect method to check the estimation results is chosen because of the technical difficulty of attaching torque measuring sensors within the clutch assembly. Through the comparison to the measured output shaft torque and careful case-by-case analysis of the estimation of each clutch torque, however, the effectiveness of the proposed observer can fully be verified.

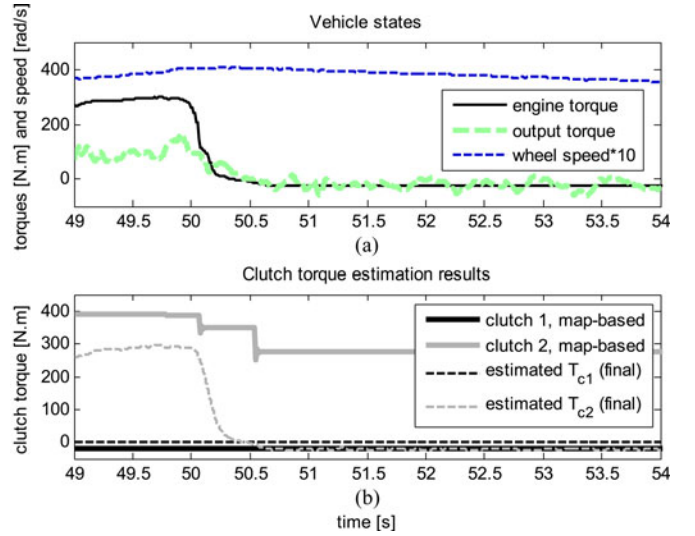


Fig. 14. Individual clutch torque estimation results during fuel cut: (a) speed measurements and (b) estimations of clutch 1 and 2 torque.

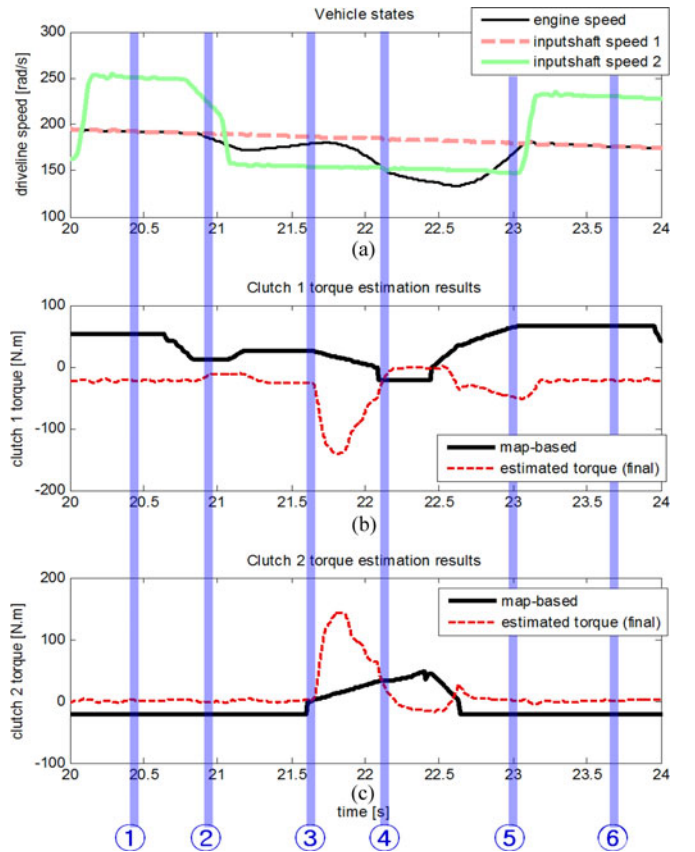


Fig. 15. Monitoring backward torque recirculation: (a) speed measurements, (b) estimation of clutch 1 torque, and (c) estimation of clutch 2 torque.

First of all, the estimations of individual clutch torque obtained by the unknown input observer alone and those obtained by the entire observer system are displayed with the simple map-based clutch torque information in Fig. 16. Again, it must be noted here that the map-based information is not shown as the credible actual clutch torque value, but instead as a rough

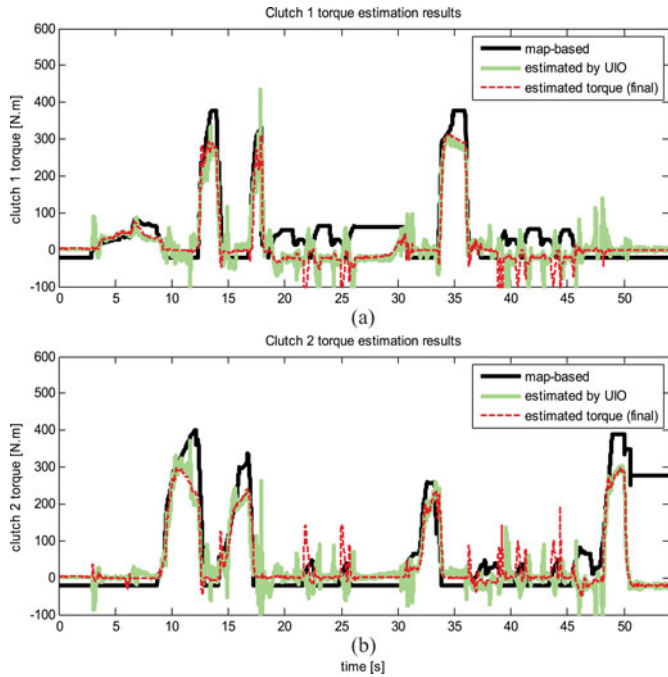


Fig. 16. Clutch torque estimation: (a) clutch 1 torque and (b) clutch 2 torque.

reference, since it merely is a set of data correlated based on the predefined map that only uses the actuator position information.

Here, the long-term stability of the clutch torque estimations is shown. Over the time period of nearly a minute, the signals successfully track the engagement and disengagement of each clutch, without any sign of divergence.

Using (48), the clutch torque estimation is converted to the output shaft torque, and is plotted in Fig. 17(a). This result based on the clutch torque estimation obtained by the proposed observer system undoubtedly gives the tracking result of the highest accuracy, when compared with the output shaft torque estimations based on the position–torque map, driveline model, and unknown input observers. The tracking error of the estimation is plotted, and is compared to that of the map-based output shaft torque data in Fig. 17(b). It apparently shows a significant amount of reduction of the estimation error.

Considering the fact that the only available conventional method to monitor each clutch torque was the clutch torque information based on the position–torque map (which is why no other estimation result of the previous work is plotted for comparison), introduction of the proposed observer that enables direct estimation of individual clutch torque is expected to bring technological advancements in the field of vehicle DCT actuator control.

The quantitative performance of the proposed observer is shown in Table I.

Here, the results in the second and third rows indicate the RMS error of the output shaft torque estimation when the observer is applied to the same scenario with the incorrect vehicle mass, and incorrect road gradient, respectively. Even when incorrect parameters are intentionally added to the models used in the observers in order to see the estimation performance under

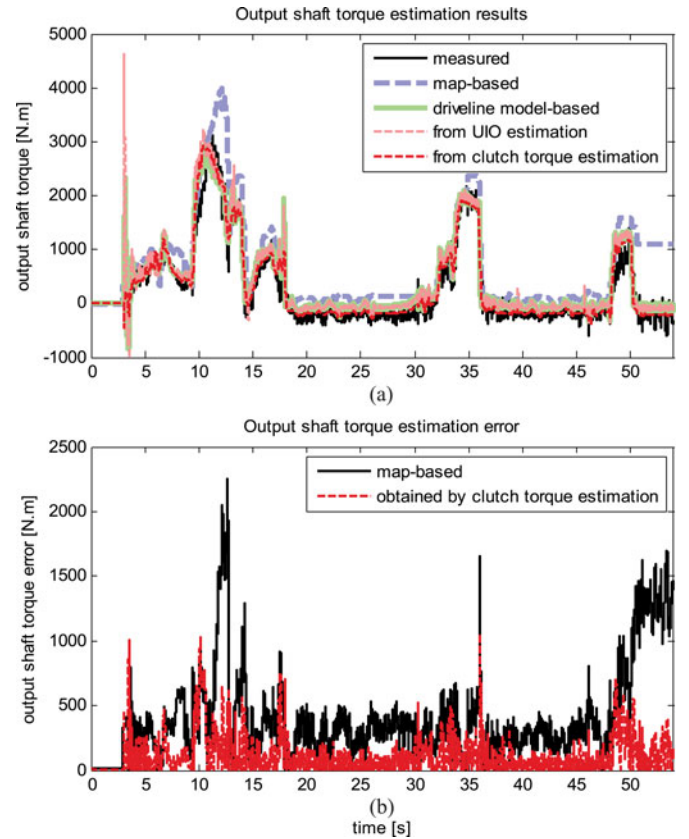


Fig. 17. Comparison of the output shaft torque estimation results: (a) output shaft torque estimations and (b) errors of the output shaft torque estimations.

TABLE I
RMS ERRORS OF THE ESTIMATED OUTPUT SHAFT TORQUE

RMS errors	Map-based	Observer estimation
Nominal model	550.06	184.01
Vehicle mass error inclusion (+1000kg)	550.06	183.96
Road gradient error inclusion (+30 deg)	550.06	184.04

model parameter uncertainty, the estimation performance is still well preserved.

Availability of the clutch torque estimation ability is more crucial during gear shifting situation, since the gear shifting control directly relates to the shift shock. The results shown in Fig. 10 reveal that the accuracy of the observer estimation is higher than that obtained based on the map. Judging from the driveline speeds shown in Fig. 10(a), what seems to be an estimation lag in (b) is rather a proof for the accurate representation of the backward torque recirculation phenomenon, which is dealt later in detail with Fig. 15.

Moreover, while the position-based or map-based actuation involves a critical limitation of having to apply the actuation force more than necessary in order to prevent clutch slip, especially during fuel cut, the direct clutch torque estimation enabled by the proposed observer allows the actuator to apply just the required amount of input to engage. This case is shown in Fig. 14, where the clutch 2 map-based torque displays an excessive

control input for the actuator of clutch 2. With the accurate clutch 2 torque estimation; however, the exact torque transmitted by each clutch is known, which can provide the amount of actuation necessary to maintain the fuel cut condition without the clutch slipping. Hence, the observer can considerably contribute to increasing the actuation efficiency of the clutch actuators.

Another major contribution of the proposed observer is the ability to monitor backward torque recirculation phenomenon internally taking place within the transmission shafts.

To validate the clutch torque estimation performance including such ability through experiments using the actual vehicle, the experiment result shown in Fig. 15 is marked with numbers ①–⑥ on the time axis, and each is analyzed in detail.

At ①, the map-based torque values in rows (b) and (c) indicate that clutch 1 is engaged and clutch 2 is disengaged. The estimation results in rows (b) and (c) indeed reveal that the clutch 2 torque is near zero and clutch 1 torque is non-zero. Here, clutch 1 torque is estimated to be a negative value. This is due to the engine friction during fuel cut, and the decreasing engine speed (thus vehicle speed, since input shaft 1 is engaged) in row (a) confirms that.

At ②, the driveline speeds and clutch 1 position indicate that clutch 1 is no longer engaged. As an expected response to this, the clutch 1 torque estimation indeed rises to zero from negative torque.

At ③, the clutch 2 position resembled by the map-based torque of clutch 2 indicates that the clutch is beginning to engage. Such event while clutch 1 is still not fully disengaged will surely cause backward torque recirculation, which is successfully monitored by the individual clutch torque estimation where clutch 1 torque suddenly decreases to reverse torque flow and clutch 2 torque suddenly rises.

This is a representative case of backward torque circulation, in which the clutch 2 torque is transmitted back onto clutch 1 rather than onto the output shaft. Monitoring this only by conventional output shaft torque observer is impossible, since the output shaft torque change during this time is minimal, as shown in Fig. 17 row (a).

The backward torque recirculation is gradually mitigated as the torque on clutch 1 is handed over onto clutch 2 while clutch 1 pulls back and clutch 2 advances. At ④, clutch 1 completely disengages, which indeed takes the clutch 1 torque estimation to zero. The engine speed continues to decrease due to the absence of negative torque flow, which causes the clutch 2 speed to be faster than the engine speed as shown in row (a), and at this exact timing, the estimated torque changes its sign as well, which confirms the validity of the estimation results.

It can be deduced from the clutch positions of the plot that at ⑤, clutch 1 is engaged while clutch 2 is fully disengaged. Here, clutch 2 torque is actually estimated to be close to zero, while clutch 1 torque is negative. The negative torque on clutch 1 is greater in magnitude than the torque estimated at ①, since the negative torque on clutch 1 at ① is induced by the vehicle inertia driving the engine (torque produced by the engine during fuel cut is negative due to internal friction) during the fully engaged phase, whereas that at ⑤ is induced during the clutch slipping

phase. As a result, the engine speed should be increasing, because the negative torque on clutch 1 is accelerating the engine, and is indeed shown to be true in row (a). The magnitude of the negative torque on clutch 1 soon decreases to the level of that at ①, when the engine speed is sufficiently accelerated and clutch 1 is fully engaged without slip. Such fuel cut condition persists at ⑥, where the states are similar to those at ①.

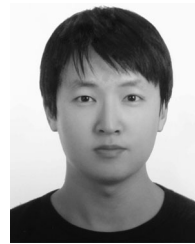
IV. CONCLUSION

This paper has proposed a novel method to effectively identify each clutch torque of the dual clutch transmission system separately. Making use of only the given set of data in the conventional production vehicles, the proposed observer system with its subcomponents of a model reference PI observer, unknown input observers, and an individual transfer shaft model-based observer interacts to give accurate torque estimation performances that are verified via experiments using an actual vehicle. Summarizing the paper, noteworthy contributions of the proposed work are the following: ability to accurately estimate the torques transmitted by each clutch separately, ability to monitor the backward torque recirculation phenomenon on real-time basis, robust output shaft torque estimation performance against various external disturbances and model uncertainty, and original signal processing methodologies to reduce noise in the torque estimation result. These original contributions are thoroughly verified through the experiments using a real car with various scenarios. Through the application of the proposed work, numerous positive impacts such as ride quality improvement by minimizing shift jerk, provision of wider range of driving style, elongated transmission life by minimizing slip and backward torque recirculation, and control input reduction (actuation efficiency improvement) are anticipated.

REFERENCES

- [1] X. Song, C. Wu, and Z. Sun, "Design, modeling, and control of a novel automotive transmission clutch actuation system," *IEEE/ASME Trans. Mechatronics*, vol. 17, no. 3, pp. 582–587, Jun. 2012.
- [2] K. Zhao, Y. Liu, X. Huang, R. Yang, and J. Wei, "Uninterrupted shift transmission and its shift characteristics," *IEEE/ASME Trans. Mechatron.*, vol. 19, no. 1, pp. 374–383, Feb. 2014.
- [3] Y. S. Yoon, S. J. Kim, and K. S. Kim, "Conceptual design of economic hybrid vehicle system using clutchless geared smart transmission," *Int. J. Automotive Technol.*, vol. 14, no. 5, pp. 779–784, Oct. 2013.
- [4] S. J. Kim, C. Song, K. Kim, and Y. S. Yoon, "Analysis of the shifting behavior of a novel clutchless geared smart transmission," *Int. J. Automotive Technol.*, vol. 15, no. 1, pp. 125–134, Feb. 2014.
- [5] J. W. Shin, J. O. Kim, J. Y. Choi, and S. H. Oh, "Design of 2-speed transmission for electric commercial vehicle," *Int. J. Automotive Technol.*, vol. 15, no. 1, pp. 145–150, Feb. 2014.
- [6] B. Matthes, "Dual clutch transmissions—Lessons learned and future potential," presented at the Transmiss. Drive Syst. Symp., 2005, Detroit, MI, USA, SAE Paper 2005-01-1021.
- [7] J. Fredriksson and B. Egardt, "Nonlinear control applied to gearshifting in automated manual transmissions," in *Proc. 39th IEEE Conf. Decision Control*, vol. 1, Sydney, Australia, 2000, pp. 444–449.
- [8] J. Horn, J. Bamberger, P. Michau, and S. Pindl, "Flatness-based clutch control for automated manual transmissions," *Control Eng. Pract.*, vol. 11, no. 12, pp. 1353–1359, 2003.
- [9] B. K. Shin, J. O. Hahn, and K. I. Lee, "Development of shift control algorithm using estimated turbine torque," SAE Paper 2000: 01-1150.
- [10] H. S. Jeong and K. I. Lee, "Friction coefficient, torque estimation, smooth shift control law for an automatic power transmission," *J. Mech. Sci. Technol.*, vol. 14, no. 5, pp. 508–517, 2000.

- [11] B. Gao, H. Chen, H. Zhao, and K. Sanada, "A reduced-order nonlinear clutch pressure observer for automatic transmission," *IEEE Trans. Control Syst. Technol.*, vol. 18, no. 2, pp. 446–453, Mar. 2010.
- [12] M. Pettersson and L. Nielsen, "Gear shifting by engine control," *IEEE Trans. Control Syst. Technol.*, vol. 8, no. 3, pp. 495–507, May 2000.
- [13] M. Pettersson, "Driveline modeling and control," Ph.D. dissertation, Dept. Electr. Eng., Linköping Univ., Linköping, Sweden, 1997.
- [14] M. Pettersson and L. Nielsen, "Diesel engine speed control with handling of driveline resonances," *Control Eng. Pract.*, vol. 11, no. 3, pp. 319–328, 2003.
- [15] L. Webersinke, L. Augenstein, and U. Kiencke, "Adaptive linear quadratic control for high dynamical and comfortable behavior of a heavy truck," SAE Tech. Paper 2008-01-0534.
- [16] K. Yi, K. Hedrick, and S. C. Lee, "Estimation of tire-road friction using observer based identifiers," *Veh. Syst. Dyn.*, vol. 31, no. 4, pp. 233–261, 1999.
- [17] B. K. Shin, J. O. Hahn, K. Yi, and K. I. Lee, "A supervisor-based neural-adaptive shift controller for automatic transmissions considering throttle opening and driving load," *KSME Int. J.*, vol. 14, no. 4, pp. 418–425, 2000.
- [18] E. Misawa and J. Hedrick, "Nonlinear observers—A state-of-the-art survey," *ASME J. Dyn. Syst., Meas. Control*, vol. 111, pp. 344–352, 1992.
- [19] C. Johnson, "Theory of disturbance-accommodating controllers," *Control Dyn. Syst.*, vol. 12, pp. 387–489, 1976.
- [20] J. Kim, J. Oh, and S. B. Choi, "Nonlinear estimation method of a self-energizing clutch actuator load," presented at the Int. Conf. Innovative Eng. Syst., Alexandria, Egypt, Dec. 2012.
- [21] Z. G. Zhao, J. L. Jiang, Z. P. Yu, and T. Zhang, "Starting sliding mode variable structure that coordinates the control and real-time optimization of dry dual clutch transmissions," *Int. J. Automotive Technol.*, vol. 14, no. 6, pp. 875–888, Dec. 2013.
- [22] K. Jinsung and S. B. Choi, "Control of dry clutch engagement for vehicle launches via a shaft torque observer," in *Proc. Amer. Control Conf.*, 2010, pp. 676–681.
- [23] M. X. Wu, J. W. Zhang, T. L. Lu, and C. S. Ni, "Research on optimal control for dry dual-clutch engagement during launch," in *Proc. Inst. Mech. Eng., J. Automobile Eng.*, 2010, vol. 224, no. 6, pp. 749–763.
- [24] V. N. Tran, J. Lauber, and M. Dambrine, "Sliding mode control of a dual clutch during launch," presented at the *2nd Int. Conf. Eng. Mech. Autom.*, Hanoi, Vietnam, Aug. 16–17 2012.
- [25] K. Han and Y. Yoon, "Clutch transmissible torque estimation for dry dual clutch transmission control," in *Proc. FISITA 2012 World Automotive Congress*, 2013, pp. 449–456.
- [26] J. Deur, V. Ivanović, Z. Herold, M. Kostelac, and H. E. Tseng, "Dry clutch control based on electromechanical actuator position feedback loop," *Int. J. Veh. Design*, vol. 60, no. 3, pp. 305–326, 2012.
- [27] J. Kim, S. B. Choi, H. Lee, J. Kang, and M. Hur, "System modeling and control of a clutch actuator system for dual clutch transmissions," in *Proc. KSAE Annu. Conf. Exhib.*, 2011, pp. 1253–1257.
- [28] X. Song and Z. Sun, "Pressure-based clutch control for automotive transmissions using a sliding-mode controller," *IEEE /ASME Trans. Mechatron.*, vol. 17, no. 3, pp. 534–546, Jun. 2012.
- [29] J. Kim and S. B. Choi, "Design and modeling of a clutch actuator system with self-energizing mechanism," *IEEE /ASME Trans. Mechatron.*, vol. 16, no. 5, pp. 953–966, Oct. 2011.
- [30] L. Glielmo, L. Iannelli, V. Vacca, and F. Vasca, "Gearshift control for automated manual transmissions," *IEEE /ASME Trans. Mechatron.*, vol. 11, no. 1, pp. 17–26, Feb. 2006.
- [31] J. Oh, J. Kim, and S. B. Choi, "Design of estimators for the output shaft torque of automated manual transmission systems," presented at the IEEE Conf. Ind. Electron. Appl., Melbourne, Australia, 2013.



Jiwon J. Oh received the Bachelor's and M.S. degrees in mechanical engineering from the Korea Advanced Institute of Science and Technology (KAIST), Daejeon, Korea, where he is currently working toward the Ph.D. degree in mechanical engineering.

His current research interests include vehicle driveline state estimation and dual clutch transmission control.



Seibum B. Choi (M'09) received the B.S. degree in mechanical engineering from Seoul National University, Seoul, Korea, the M.S. degree in mechanical engineering from the Korea Advanced Institute of Science and Technology (KAIST), Daejeon, Korea, and the Ph.D. degree in control from the University of California, Berkeley, CA, USA, in 1993.

From 1993 to 1997, he was involved in the development of automated vehicle control systems at the Institute of Transportation Studies, University of California. During 2006, he was with TRW, Warren, MI, USA, where he was involved in the development of advanced vehicle control systems. Since 2006, he has been with the faculty of the Mechanical Engineering Department, KAIST. His current research interests include fuel-saving technology, vehicle dynamics and control, and active safety systems.